Effects of Dispersion and Arrangement of Clay on Thermal Diffusivity of Polyimide-Clay Nanocomposite Film

Masaki Kakiage,* Shinji Ando

Department of Chemistry and Materials Science, Tokyo Institute of Technology, Ookayama 2-12-1-E4-5, Meguro-ku, Tokyo 152-8552, Japan

Received 22 April 2010; accepted 1 July 2010
DOI 10.1002/app.33034
Published online 22 September 2010 in Wiley Online Library (wileyonlinelibrary.com).

ABSTRACT: Polymer-clay nanocomposites are well-known high-performance materials with a superior tensile modulus. However, in the case of composites with polyimide (PI), additional functions require study because PI is a high-performance material in itself. Significant enhancement of thermal conductivity, which is closely related to the state of clay dispersion, is expected for a polymer-clay nanocomposite. In this study, variations in the thermal diffusivity of PI-clay nanocomposite films prepared by different methods were investigated. The thermal diffusivity of PI-clay nanocomposite film increased at low clay content only when unmodified clay was used, where the clay morphology was a layered structure dispersed on a nanometer scale. Moreover, the thermal diffusivity could be enhanced by controlling the tensile stress induced by spontaneous shrinkage of the film during thermal imidization. These results demonstrated that the thermal diffusivity of PI-clay nanocomposite films is significantly affected by the dispersion and/or arrangement states of the clay. © 2010 Wiley Periodicals, Inc. J Appl Polym Sci 119: 3010–3018, 2011

Key words: polyimide; clay; nanocomposites; layered structure; thermal diffusivity

INTRODUCTION

Polymer-inorganic nanocomposites are becoming important materials nowadays. In particular, polymer-clay nanocomposites are typical high-performance materials with a superior tensile modulus.[1–9] Mechanical properties, heat resistance, and gas permeability can be improved by the nanocomposite technique for clay with low clay content because a clay platelet has a high-aspect ratio, and the clay dispersion state greatly affects the pathway of a diffusing gas[10] and volatile decomposition products.[11] Polyimide (PI)-clay nanocomposites can be prepared by using a common solvent method, in which poly(amic acid) (PAA), a precursor of PI, and clay are separately dissolved in the same kinds of organic solvents, followed by blending both solutions.[10,12–22] Most of the studies on PI-clay nanocomposites have been concerned with their mechanical properties; however, in the case of composites with PI, additional functions require study because PI is an inherently high-performance material with superior mechanical properties, good flexibility, and high thermal and chemical stability.[23] Therefore, we focus our attention on the thermal conductivity of PI-clay nanocomposite films as a novel function.

A few investigations have been reported on the thermal conductivity in polymer-clay nanocomposites, in which a lowering of thermal conductivity was recognized.[24–26] However, the enhancement of thermal conductivity, which should be closely related to the dispersion and aggregation state of clay, is highly expected for polymer-clay nanocomposites under controlled conditions. In particular, the thermal conductivity in nanocomposite films decreased with exfoliated clay platelets but increased with higher clay content (over 15 wt %) due to the presence of clay agglomerates.[26] This sounds reasonable because exfoliated clay platelets not only dramatically increase the clay surface, resulting in larger interfacial thermal resistance, but also reduce the thermal conductivity of clay itself by one to three orders of magnitude due to the size effect.[26–29] This knowledge indicates that enhancement of the thermal conductivity of polymer-clay nanocomposites is fairly difficult, but it could be possible by controlling the "dispersion" and "arrangement" states of clay in the polymer matrix. Therefore, in this study, variations in the thermal diffusivity of PI-clay

**Present address:* Department of Applied Chemistry, Saitama University, 255 Shimo-Okubo, Sakura-ku, Saitama 338-8570, Japan.
Correspondence to: S. Ando (sando@polymer.titech.ac.jp).

nanocomposite films prepared by different methods were extensively investigated.

First, we attempted to disperse unmodified clay into a PI matrix for dispersion control because the presence of clay agglomerates is necessary or advantageous to enhance thermal conductivity. An increase in thermal conductivity could be achieved with low clay content if the clay is homogeneously dispersed in a polymer matrix while maintaining its original layered structure. However, nano-ordered dispersion of unmodified clay is very difficult because an inorganic clay mineral consisting of silicate layers has little affinity for organic substances, that is, matrix polymers and polar organic solvents. Hence, organically modified clay (organoclay) has been widely used for polymer-clay nanocomposites due to the good dispersion of single clay platelets on a nanometer scale. Unfortunately, however, this advantage brings about the opposite effect to the thermal conductivity of nanocomposite films owing to an increase in interfacial thermal resistance. In addition, there is concern about the destruction of the clay by mechanical dispersion like ultrasonication.[30] On the other hand, several methods for direct dispersion of unmodified clay into a polymer matrix have been proposed.[31–34] Among them, we took notice of the solvent-exchange method,[33,34] which enables homogeneous dispersion of unmodified clay in an organic solvent. This is very advantageous because PI-clay nanocomposites should be prepared using a common solvent method.

PI films are usually prepared by thermal imidization via PAA films formed on substrates, because PI is generally insoluble in organic solvents. During the imidization process, large tensile stress is induced on the PI films from substrates due to the spontaneous shrinkage of PI films, and PI chains are thus oriented in the film plane (in-plane direction).[35] The degree of in-plane chain orientation can be controlled by releasing tensile stress from a fixed condition, that is, a PAA film peeled from the substrate and thermal imidized under an off-substrate condition exhibits small in-plane/out-of-plane birefringence, which corresponds to a lower degree of in-plane orientation. Further, the arrangement of clay dispersed in a PI matrix can be controlled by using the spontaneous shrinkage behavior during the thermal curing of PI-clay films. This approach utilizes the characteristic behavior of PI films prepared from a PAA.

EXPERIMENTAL SECTION

Materials

The s-BPDA/ODA PI used in this study was prepared from 3,4,3′,4′-biphenyltetracarboxylic dianhydride (s-BPDA) and 4,4′-oxydianiline (ODA) (Fig. 1), which exhibits the highest thermal diffusivity along the out-of-plane direction ($\alpha_\perp$) among 21 kinds of aromatic and semiaromatic PIs.[36–38] s-BPDA, purchased from Wako Pure Chemicals Industries, Japan, was dried at 170°C for 12 h under vacuum before use. ODA, also purchased from Wako, was purified by recrystallization in tetrahydrofuran, followed by sublimation under reduced pressure. Clay (montmorillonite, Kunipia F) was supplied by Kunimine Industries Co., Japan. The cation exchange capacity (CEC) of this clay was 110 meq/100 g. The initial clay material (Kunipia F), dispersed in distilled water, was combined with an appropriate amount (equimolar to the CEC of the clay) of dimethyldistearylammonium chloride, $[(C_{18}H_{37})_2N^+(CH_3)_2]Cl^-$. This solution was stirred to give an organically modified clay precipitate, followed by filtering, washing, and drying at 60°C. The resulting solid cake was powdered for sample supply.

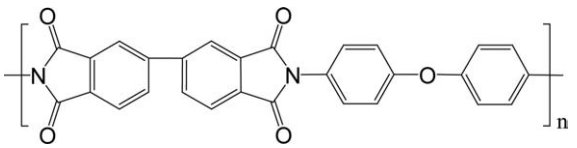

Figure 1 Molecular structure of s-BPDA/ODA polyimide.

Preparation of PAA-clay solution

A PAA solution was prepared by mixing an equimolar amount of dianhydride (s-BPDA) and diamine (ODA) in *N*,*N*-dimethylacetamide (DMAc, purchased from Aldrich, Japan, anhydrous grade). Dianhydride was added to the diamine solution in a nitrogen-purged glove box, followed by stirring in a tightly sealed reaction flask at room temperature (RT) for 1 day. The clay solution was prepared by the solvent-exchange method[33,34] using a common solvent, DMAc. Clay powder (3 wt % based on PI) was fully dispersed in distilled water (clay-water suspension), followed by the addition of an equal amount of DMAc and stirring at RT for 1 day (clay-water-DMAc suspension). The clay was homogeneously dispersed in a mixture of water and DMAc. Fully exfoliated dispersion of the clay in DMAc was prepared by subsequent distillation of water under reduced pressure (clay-DMAc suspension). The suspension thus obtained was homogeneous and semitransparent without colloidal precipitation, which is the same state as a clay-water suspension in appearance. In contrast, the clay was precipitated in the case of direct blending of clay powder with DMAc, even after adequate stirring. A separately prepared PAA solution and a clay-DMAc suspension were mixed by stirring at RT for 1 day (PAA-clay suspension). An agitated PAA-clay suspension was prepared by further strong agitation of the PAA-clay suspension using a

THINKY Mixer ARE-310, in which the sample was rotated at 2000 rpm for 7 min and deaerated at 2200 rpm for 2 min. Meanwhile, organoclay was directly added to DMAc and stirred at RT for 1 day, followed by blending with the PAA solution, as described above (PAA-organoclay suspension).

Film preparation

PI (s-BPDA/ODA) without clay and four kinds of PI-clay nanocomposite films were prepared by thermal imidization of a PAA solution and PAA-clay suspensions. The PAA solution and suspensions were spin-coated onto silica substrates, dried at 70°C for 1 h, and thermally imidized at 350°C for 1.5 h under nitrogen gas flow at a heating rate of 5°C/min. In this study, the nanocomposite films prepared from (i) a PAA-clay suspension, (ii) an agitated PAA-clay suspension, and (iii) a PAA-organoclay suspension are called "PIC-1," "PIC-2," and "PIC-3," respectively. All films were cured on silica substrates. On the other hand, a nanocomposite film prepared from a PAA-clay suspension and cured under a no-tensile-stress condition is called "PIC-4." Here, a PAA-clay film was peeled from the substrate after drying, and it was attached onto the substrate again with small pieces of PI tape, followed by thermally imidization. The average thickness of these nanocomposite films was 30 μm. The films thus obtained were easily peeled off from the substrates after cutting the edges. Here, no self-supporting film was obtained when the film was prepared from a directly blended suspension of unmodified clay with DMAc in a PAA solution.

Measurements

X-ray diffraction (XRD) measurements were performed by using a Rigaku MiniFlex operating at 35 kV and 15 mA with nickel-filtered Cu Kα radiation. The scan was carried out in the 2θ range of 3–40° with an angle interval of 0.01° and a scan speed of 1°/min. Two-dimensional XRD measurements for edge-view observation were performed by using a Rigaku UltraX18 X-ray generator operating at 40 kV and 50 mA with nickel-filtered Cu Kα radiation and a flat imaging plate. Polarized attenuated total reflectance (ATR) Fourier transform infrared (FT-IR) spectra of films were measured using a Nicolet Avatar 320 spectrometer attached with a Spectra-Tech Thunderdome single reflection ATR attachment (incident angle is 45°) and an aluminum wire-grid ZnSe polarizer. The internal reflection element in the ATR attachment is made of germanium crystal with a refractive index of 4.0. A_{TE} denotes the polarized absorbance of reflected light for the transverse electric (TE) direction that is parallel to the film surface ($=A_{X(Y)}$), and A_{TM} denotes that for the transverse magnetic (TM) direction that is perpendicular to the film surface ($=A_{Y(X)} + A_Z$). We defined the differential absorbance (ΔA) as $A_{TM} - 2A_{TE}$ because A_{TM} is double of A_{TE} when the absorption of film is isotropic. Transmission electron microscopy (TEM) observations of the films were conducted with a JEOL JEM-200CX electron microscope operated at 200 kV and a JEOL JEM-1010BS electron microscope operated at 100 kV. The samples were embedded in an epoxy resin, and the assembly was cut into thin sections 55–80 nm thick for TEM observation. Thermal diffusivity, which is a predominant factor in thermal conductivity, was selected for evaluation of the thermal conductivity of the films. The thermal diffusivity of the films along the thickness direction ($\alpha_\perp$) at RT was measured by temperature wave analysis[36–43] using an ai-Phase Mobile 1u (ai-Phase Co., Japan), in which the sensing probe size was 0.25 × 0.5 mm. In the analysis, three values were measured for each film, and the average value was recorded as the thermal diffusivity.

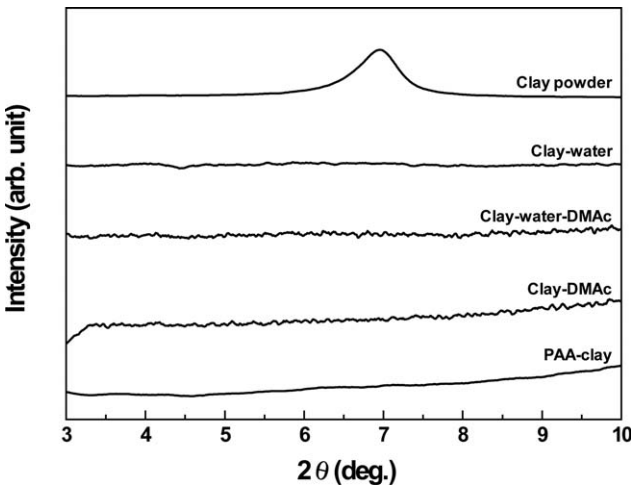

Figure 2 Comparison of the XRD patterns recorded during PAA-clay suspension preparation using the solvent-exchange method. The XRD pattern of clay powder is also plotted as a reference.

RESULTS AND DISCUSSIONS

The variations in the clay dispersion states were first investigated using XRD measurements. Figure 2 exhibits the XRD patterns recorded in the process of preparing the PAA-clay suspension. The basal spacing of clay powder, estimated from the peak position, was ~ 1.2 nm. No clay reflection was detected during the solvent-exchange processes, that is, clay-water, clay-water-DMAc, and clay-DMAc suspensions, although a (100) reflection of the clay appeared for the directly blended suspension of clay in DMAc (not shown). Furthermore, no characteristic reflection of the clay was observed for the XRD pattern of the PAA-clay suspension after blending the

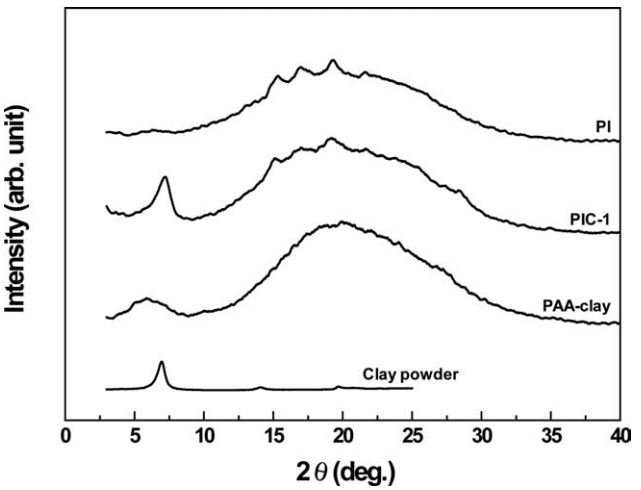

Figure 3 Comparison of the XRD patterns for PAA-clay and PIC-1 films. The patterns of clay powder and PI film without clay are also plotted as references.

PAA solution and clay-DMAc suspension. This means that the clay was fully exfoliated without forming a layered structure even in the organic solvent (DMAc) and with PAA chains in the suspension state. Figure 3 exhibits the XRD patterns recorded during the thermal imidization of a PAA-clay film. The broad (001) reflection peak appearing at $2\theta = 6^\circ$ for PAA-clay film indicates that the layered clay structure was reconstructed in the film during drying at 70°C. The basal spacing was ~ 1.5 nm, which is larger than that of the original clay (1.2 nm). After thermal imidization at 350°C (PIC-1 film), the clay (001) reflection peak became sharp and shifted to a higher 2θ of 7°, which corresponds to that for the original clay powder. This indicates that the clay morphology in the PIC-1 film is a layered structure, and the original layered structure was recovered from the exfoliated clay platelets during the drying of the solvent. Furthermore, densification of the layered structure was accelerated during thermal imidization at elevated temperatures.

A model for the structural formation in PI-clay nanocomposite film during imidization is illustrated in Figure 4. First, the clay platelets are uniformly dispersed in the PAA-clay suspension, but these clay platelets generate nano-agglomerates having a "house-of-cards" structure, in which the edge-to-edge and the edge-to-face interactions between the dispersed platelets form a kind of percolation structure.[44–47] Thus, with evaporating water and solvent from PAA-clay suspension during drying and thermal imidization, the local concentration of the clay was increased and the interactions between the clay platelet and ambient organic materials (DMAc and PAA molecules) were weakened. Moreover, the clay platelets in the film were gradually immobilized with the progress of imidization because the structure of PI main chains is more rigid than that of PAA. These chemical and spatial restraint effects reduce the distance between the clay platelets with the collapse of the house-of-cards structure and lead to recovery from the exfoliated clay platelets to the original layered structure. Chen et al.[20] reported the structural change in PI-clay and PI-organoclay nanocomposite films that occurred during thermal imidization. The variation in the interlayer distance observed in the PI-organoclay film is similar to that observed in this study. Namely, the clay (001) reflection appeared with solvent drying, and the clay interlayer distance was decreased by imidization. This clearly indicates that unmodified clay platelets prepared by the solvent-exchange method have preferable interactions between the clay platelet and ambient organic materials, which has an effect similar to organically modified clay. However, in this study, the clay interlayer distance was recovered to the same extent as the original clay after imidizaiton because unmodified clay was used. TEM observation was carried out to characterize the clay dispersion state in PIC-1 film, as shown in Figure 5. No clay agglomerates are observed on a micrometer scale, which is very unusual behavior for conventional polymer-unmodified clay nanocomposites. The domain size of the clay is ~ 30 nm along the thickness direction, indicating that the dispersed domain has a layered structure consisting of several platelets, not of a single platelet (~ 1 nm). Therefore, a dispersion morphology with both remarkable nanosize dispersion and a layered structure with the original clay interlayer distance was newly achieved in the PI-clay nanocomposite film using unmodified clay with the solvent-exchange method.

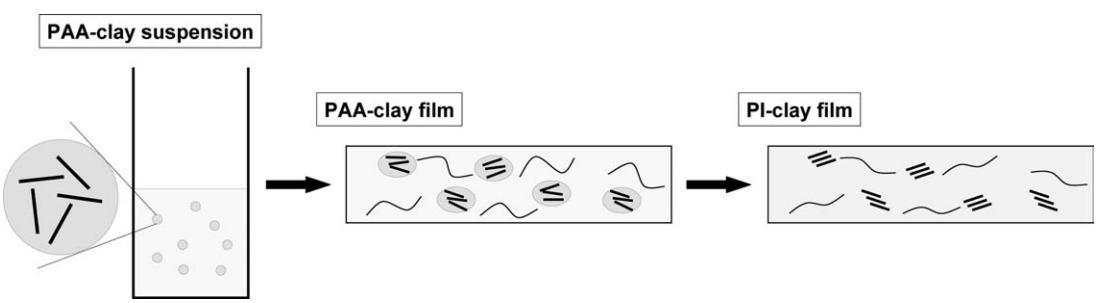

Figure 4 Structural formation model for PI-clay nanocomposite film.

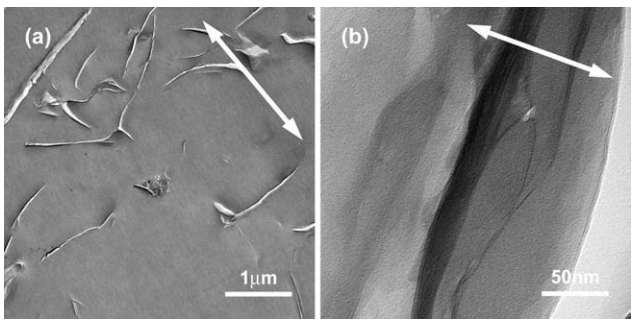

Figure 5 TEM images of PIC-1 film. The arrows indicate the thickness direction. The dark lines correspond to clay platelets. The clay domains in (a) are enlarged in (b).

The thermal diffusivity along the out-of-plane direction ($\alpha_\perp$) of the PIC-1 film was estimated to be 18.47×10^{-8} m^2/s, which is higher than that for the PI film without clay (16.00×10^{-8} m^2/s). This is noteworthy because thermal conductivity was improved in the clay nanocomposite with low clay content, 3 wt %, whereas more than 15 wt % clay content was needed in a previous report.[26] The major difference between previous studies and the present one is the dispersion state of the clay. Previous research covered only polymer-organoclay nanocomposites, where the clay dispersion state was essentially exfoliated and/or intercalated. Consequently, the clay platelets served as a resistance to heat transmission, and so thermal conductivity decreased. In contrast, a layered structure was reconstructed in the PIC-1 film. The layered clay structure enhances thermal conductivity. Furthermore, a clay agglomerate having a house-of-cards structure in the PAA-clay solution was expected to be involved in a percolation network, which leads to an increase in thermal conductivity with low clay content. These findings point to the fact that the thermal conductivity of a polymer-clay nanocomposite is essentially dominated by the clay dispersion state.

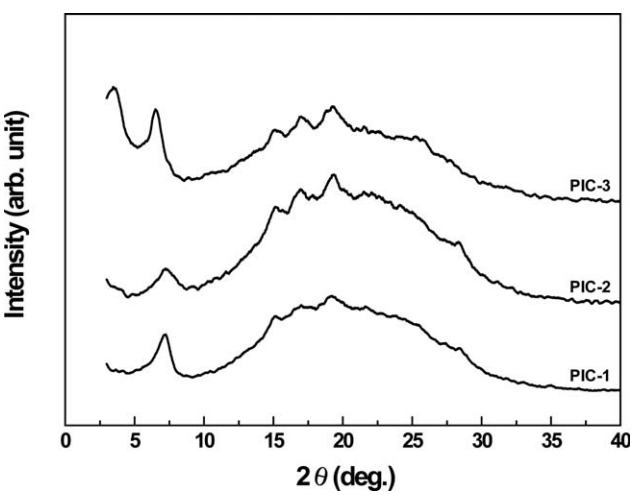

Figure 6 Comparison of the XRD patterns for PIC-1, PIC-2, and PIC-3 films.

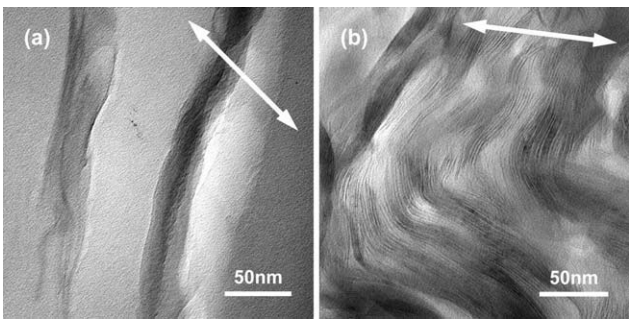

Figure 7 TEM images of (a) PIC-2 and (b) PIC-3 films.

Considering the effect of the clay dispersion morphology on thermal diffusivity, two approaches were carried out: one was strong agitation of a PAA-clay suspension using a mechanical mixer (PIC-2 film), and the other was a PI-organoclay nanocomposite (PIC-3 film). Comparing the XRD patterns (Fig. 6), the clay (001) reflection of PIC-2 film is broader than that of PIC-1 film, indicating a decrease in dispersed clay domain size by the mechanical mixing. On the other hand, additional appearance of clay (001) reflection at a lower 2θ for PIC-3 film reveals the formation of partial intercalated structure with wider basal spacing of $\sim$ 2.5 nm. Figure 7 presents the TEM images of these films. A layered clay structure similar to PIC-1 film is observed for the former, but the clay domain size in the thickness direction is partially smaller [15–25 nm, Fig. 7(a)]. In contrast, a typical intercalated structure with clay platelets, which is entirely different from PIC-1 and PIC-2 films, was observed for PIC-3 film [Fig. 7(b)]. This structure is frequently observed in conventional polymer-organoclay nanocomposites. The thermal diffusivities ($\alpha_\perp$) of these films with different clay morphologies are summarized in Figure 8. The $\alpha_\perp$ value of PIC-2 film with layered but thin clay structures is comparable to that of PI film without clay but lower than that of PIC-1 film, indicating that a

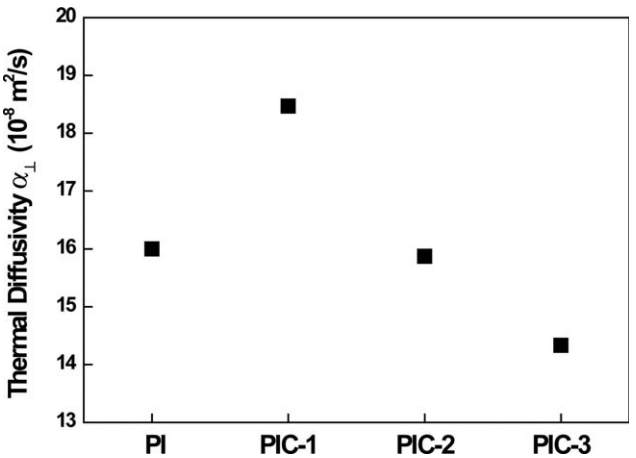

Figure 8 Thermal diffusivities ($\alpha_\perp$) of PI-clay nanocomposite films with different clay morphologies.

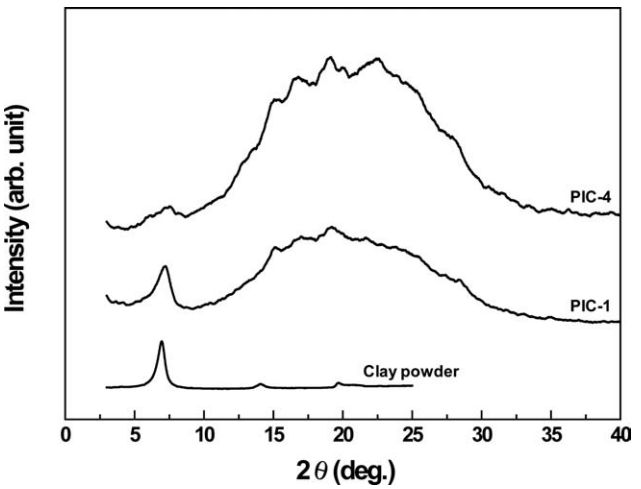

Figure 9 XRD patterns of PIC-1 and PIC-4 films. The pattern of clay powder is also plotted as a reference.

certain amount of layer thickness is required to overcome the large interfacial thermal resistance of clay. A further decrease in $\alpha_\perp$ was observed for PIC-3 film having an intercalated structure. Thus, only the effect of interfacial thermal resistance of clay was added to polymer-clay nanocomposites with exfoliated and/or intercalated clay morphologies. Another possibility for the decrease in $\alpha_\perp$ is the structural imperfection of clay because structural regularity affects the lattice vibrations in nonmetallic solids, that is, phonons are scattered at the lattice defects and interfaces. On this point, the formation of the original layered structure of clay was advantageous to increase the $\alpha_\perp$ of PI-clay nanocomposites. Comparing the clay dispersion morphology evaluated by TEM observation with the experimental values of $\alpha_\perp$, a trend is very clear; that is, $\alpha_\perp$ decreases with the transformation of clay dispersion from a layered structure to a single-clay-platelet structure. These results demonstrate that enhancement of thermal conductivity for a polymer-clay nanocomposite requires homogeneous dispersion of a layered clay structure having an appropriate layer thickness and a percolation network.

A very characteristic factor of clay is the significant anisotropy of its thermal conductivity, which is attributed to the high aspect ratio (200–2000)[2] and large interfacial thermal resistance of clay platelets. Thus, it is assumed that the thermal properties of a polymer-clay nanocomposite can be controlled by varying the clay arrangement. In this study, we attempted to change the clay arrangement by using the spontaneous shrinkage phenomenon of PAA films during thermal imidization.[35,48] Figure 9 exhibits the XRD pattern of PIC-4 film cured under a no-tensile-stress condition. Compared with PIC-1 film cured on the substrate, the clay (001) reflection of the former is weaker and broader than the latter, though the peak position is the same. This indicates the changes in the clay arrangement and/or the disarrangement of the layered clay structure. Figure 10 presents the TEM images of PIC-4 film. Since the thickness of layered clay [$\sim$ 30 nm, Fig. 10(b)] is similar to that in PIC-1 film [Fig. 5(b)], these films have the same clay dispersion structure, that is, a dispersed layered structure together with the original interlayer distance. However, an important difference is recognizable between the films regarding the clay arrangement in the PI matrix. Layered clays are arranged parallel to the film surface (i.e., an "in-plane arrangement") for PIC-1 film [Fig. 5(a)], which is popular in spin-coated polymer-clay nanocomposite films. In contrast, layered clays are partially arranged normal to the film surface (i.e., a "partial out-of-plane arrangement") for PIC-4 film [Fig. 10(a)]. This means that the clay arrangement can be varied by spontaneous shrinkage during thermal imidization, without disarrangement of the layered structure. The orientation state of a polymer-clay nanocomposite film could be evaluated using polarized FT-IR measurement.[49–54] It should be noted that the 1080 cm^{-1} band of a montmorillonite is assigned to the "out-of-plane" Si-O stretching vibration mode, perpendicular to a clay platelet,[55] which is sensitive to the layered arrangement and exhibits significant dichroism by polarized FT-IR measurement.[51,52,54–57] Figure 11(a,b) exhibit the polarized ATR FT-IR spectra and the differential absorbance (ΔA) spectra of PI, PIC-1, and PIC-4 films. The ΔA values of out-of-plane Si-O mode at 1080 cm^{-1} are opposite between PIC-1 and PIC-4 films, that is, PIC-1 film is positive but PIC-4 film is negative, meaning that the amount of perpendicular-arranged out-of-plane Si—O bonds for PIC-1 film is larger than that for PIC-4 film. These imply the transformation of the clay arrangement from in-plane (PIC-1 film) to out-of-plane (PIC-4 film) direction. These differences were analyzed by edge-view XRD measurements, a useful analytical method to evaluate the clay orientation along the thickness direction.[5,58–60] The edge-view images of PIC-1 and PIC-4 films are respectively, presented

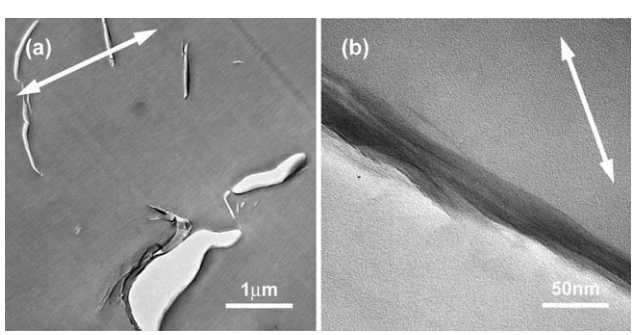

Figure 10 TEM images of PIC-4 film. The clay domains in (a) are enlarged in (b).

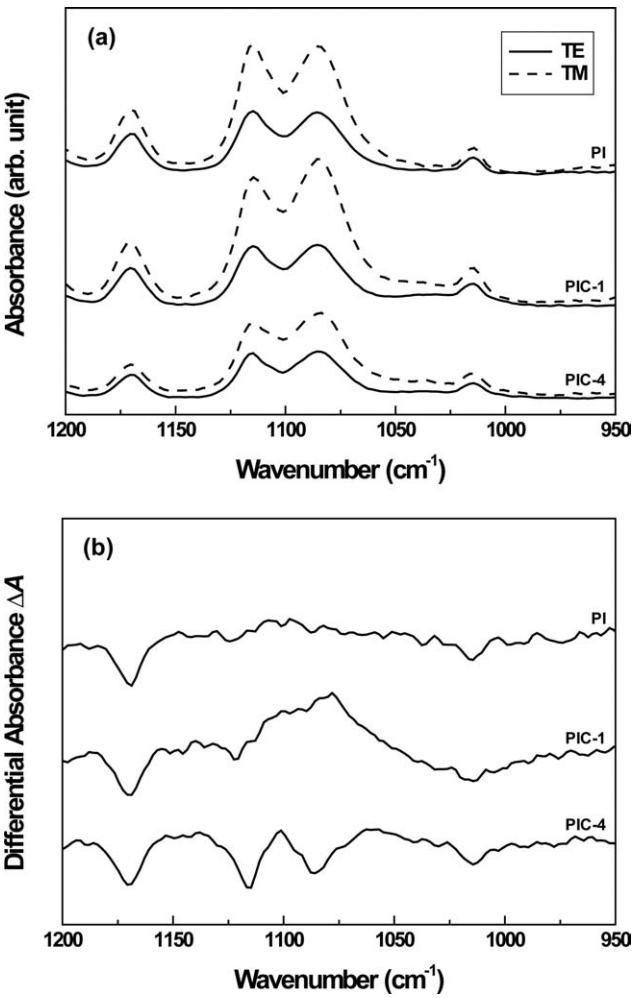

Figure 11 (a) Polarized ATR FT-IR spectra for PI, PIC-1, and PIC-4 films. (b) Differential absorbance (ΔA) spectra estimated from TE and TM spectra in Figure 11(a).

in Figure 12(a,b). Clay (001) reflections with an arc shape were observed parallel to the thickness direction for both films, indicating that the layered direction of clay is mainly parallel to the thickness direction; that is, layered clay had an in-plane arrangement. However, the clay (001) reflection of PIC-4 film is more isotropic than that of PIC-1 film, indicating that the clay arrangement transformed from in-plane to out-of-plane in the free-shrinkage film. The clay arrangements were quantitatively analyzed by comparing the azimuthal profiles extracted along the azimuthal angle at the clay (001) reflection peak of the edge-view images of PIC-1 and PIC-4 films, as respectively shown in Figure 12(a,b). The azimuthal profiles are plotted in Figure 12(c), in which a clear broadening of the clay (001) reflection peak is observed. The peak of PIC-4 film is broader than that of PIC-1 film. For a detailed analysis, the full width at half maximum (FWHM) of the clay (001) reflection peaks were evaluated from the peak separation using the Gaussian function in the azimuthal profiles, as shown in Figure 12(c). The degree of clay orientation in the film plane (D) was evaluated from eq. (1).

$$D = \frac{180 - \mathrm{FWHM(deg.)}}{180} \tag{1}$$

The D values thus obtained were 0.73 and 0.60 for PIC-1 and PIC-4 films, respectively, which indicate that the transformation of the clay arrangement from the in-plane (PIC-1 film) to the out-of-plane direction (PIC-4 film) was developed by the spontaneous shrinkage of PI films during thermal imidization.

The thermal diffusivities ($\alpha_\perp$) and the degree of clay orientation in the film plane (D) observed for the PIC-1 and PIC-4 films are summarized in Figure 13. A higher increase in $\alpha_\perp$ was achieved for the latter than the former, which accords with the decrease in the in-plane orientation of clay; that is, the layered clay has a higher out-of-plane arrangement. In other words, a transformation of the clay

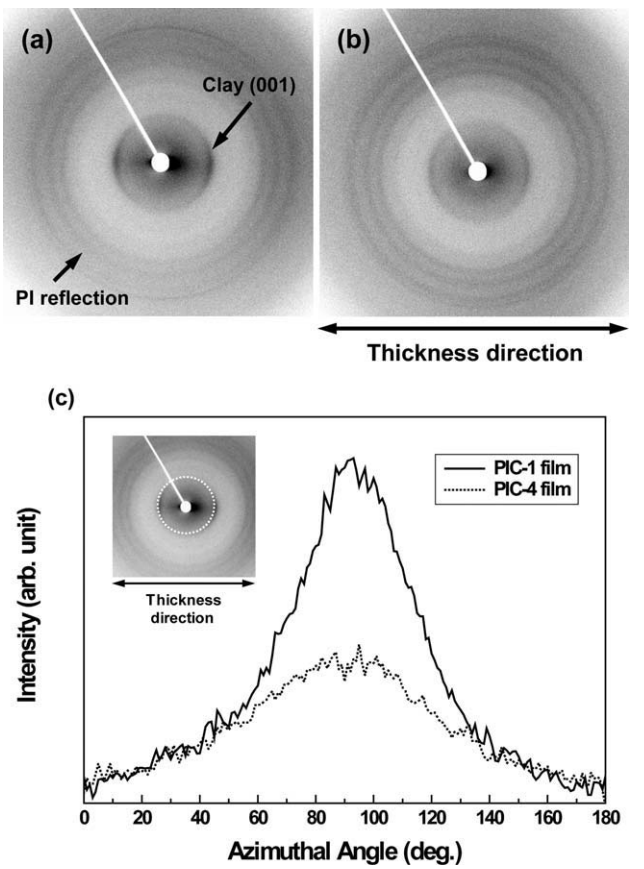

Figure 12 Edge-view images of (a) PIC-1 and (b) PIC-4 films. The thickness direction is horizontal in the images. (c) Azimuthal profiles extracted along the azimuthal angle at the clay (001) reflection peak for the edge-view images. The schematic of azimuthal extraction of the profile is represented by the white dotted line in the inset image.

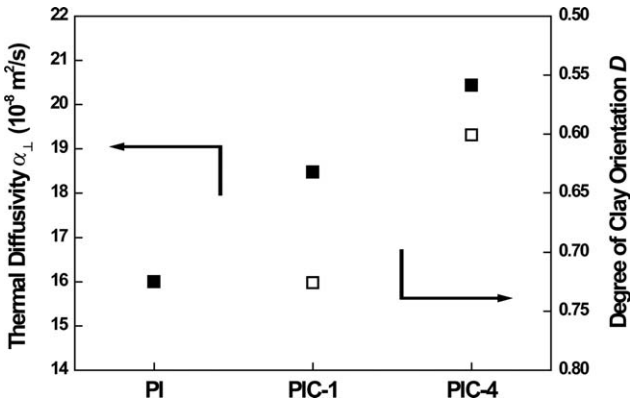

Figure 13 Thermal diffusivities ($\alpha_\perp$) (filled square) and degrees of clay orientation in the film plane (D) (open square) of PI, PIC-1, and PIC-4 films.

arrangement leads to an increase in $\alpha_\perp$. This result demonstrates that the thermal conductivity of a PI-clay nanocomposite film can be enhanced by controlling the tensile stress induced by shrinkage during thermal curing. The thermal resistance of clay in a nanocomposite film decreases with an increase in the out-of-plane orientation of layered clay due to the large aspect ratio of the clay platelet. Moreover, thermal conduction paths are partially formed along the out-of-plane orientation of layered clay involving a percolation network because the paths are generated parallel to the clay surface in a clay platelet. The functions of these aspects lead to the enhancement of thermal diffusivity of PIC-4 film.

In summary, a new material design for a PI-clay nanocomposite film with high thermal diffusivity was attempted in this study, using the solvent-exchange method and the spontaneous shrinkage of PI films during thermal imidization. The function, that is, thermal diffusivity, was developed only by using unmodified clay because the solvent-exchange method introduced the dispersion of layered clay and generated a percolation network through the spontaneous shrinking, which introduced the transformation of the clay arrangement from the in-plane to the partially out-of-plane direction. Control of the dispersion and/or arrangement of clay causes significant changes in the thermal diffusivity of PI-clay nanocomposite film. Consequently, these approaches are promising methodologies for building a new polymer-clay nanocomposite exploiting the intrinsic characteristics of bulk clay.

CONCLUSIONS

The effects of clay dispersion and arrangement on the thermal diffusivity ($\alpha_\perp$) of PI-clay nanocomposite films were investigated. Unmodified clay was fully exfoliated in DMAc and PAA solutions using the solvent-exchange method, although the exfoliated clay platelets recovered the original layered structure during thermal imidizaiton due to the decrease in interaction between the clay platelet and ambient organic substances. The clay morphology obtained for PIC-1 film was a "dispersed layered structure" on a nanometer scale having an original interlayer distance without agglomerates. The $\alpha_\perp$ of PIC-1 film with a dispersed layered structure clay morphology was higher than that of PI film without clay, whereas the $\alpha_\perp$ of PIC-3 film prepared from organoclay having an intercalated structure morphology was lower. Thereby, the $\alpha_\perp$ of PI-clay nanocomposite film increased with lower clay content only when unmodified clay was used. Furthermore, the $\alpha_\perp$ of PIC-4 film was markedly enhanced because the clay arrangement was transformed from the in-plane to the partially out-of-plane direction by the spontaneous shrinkage of the film during thermal imidization. These results demonstrate that the thermal diffusivity of PI-clay nanocomposite films can be controlled by changing the dispersion and/or arrangement states of clay.

The authors appreciate Jun Koki (Center for Advanced Materials Analysis, Tokyo Institute of Technology) for the TEM observations. M. Kakiage expresses his gratitude for the support by the Japan Society for the Promotion of Science (JSPS) Research Fellowships for Young Scientists and a Grant-in-Aid for the JSPS Fellows.

References

1. LeBaron, P. C.; Wang, Z.; Pinnavaia, T. J Appl Clay Sci 1999, 15, 11.
2. Pinnavaia, T. J.; Beall, G. W. Polymer-Clay Nanocomposites; Wiley: New York, 2000.
3. Alexandre, M.; Dubois, P. Mater Sci Eng R-Rep 2000, 28, 1.
4. Sinha Ray, S.; Okamoto, M. Prog Polym Sci 2003, 28, 1539.
5. Usuki, A.; Hasegawa, N.; Kato, M. Adv Polym Sci 2005, 179, 135.
6. Okada, A.; Usuki, A. Macromol Mater Eng 2006, 291, 1449.
7. Paul, D. R.; Robeson, L. M. Polymer 2008, 49, 3187.
8. Pavlidou, S.; Papaspyrides, C. D. Prog Polym Sci 2008, 33, 1119.
9. Choudalakis, G.; Gotsis, A. D. Eur Polym Mater 2009, 45, 967.
10. Yano, K.; Usuki, A.; Okada, A.; Kurauchi, T.; Kamigaito, O. J.; Polym Sci Part A: Polym Chem 1993, 31, 2493.
11. Chen, G.; Liu, S.; Chen, S.; Qi, Z. Macromol Chem Phys 2001, 202, 1189.
12. Lan, T.; Kaviratna, P. D.; Pinnavaia, T. J Chem Mater 1994, 6, 573.
13. Yano, K.; Usuki, A.; Okada, A. J. Polym Sci Part A: Polym Chem 1997, 35, 2289.
14. Tyan, H.-L.; Liu, Y.-C.; Wei, K.-H. Chem Mater 1999, 11, 1942.
15. Tyan, H.-L.; Liu, Y.-C.; Wei, K.-H. Polymer 1999, 40, 4877.
16. Gu, A.; Kuo, S.-W.; Chang, F.-C. J Appl Polym Sci 2001, 79, 1902.
17. Chang, J.-H.; Park, K. M.; Cho, D.; Yang, H. S.; Ihn, K. J Polym Eng Sci 2001, 41, 1514.
18. Agag, T.; Koga, T.; Takeichi, T. Polymer 2001, 42, 3399.
19. Zhang, Y.-H.; Wu, J.-T.; Fu, S.-Y.; Yang, S.-Y.; Li, Y.; Fan, L.; Li, R. K.-Y.; Li, L.-F.; Yan, Q. Polymer 2004, 45, 7579.
20. Chen, H.-S.; Chen, C.-M.; Chang, G.-Y.; Lee, S.-Y. Mater Chem Phys 2006, 96, 244.

21. Mya, K. Y.; Wang, K.; Chen, L.; Lin, T. T.; Pallathadka, P. K.; Pan, J.; He, C. Macromol Chem Phys 2008, 209, 643.
22. Lai, M.-C.; Jang, G.-W.; Chang, K.-C.; Hsu, S.-C.; Hsieh, M.-F.; Yeh, J.-M. J Appl Polym Sci 2008, 109, 1730.
23. Sroog, C. E. J Polym Sci Macromol Rev 1976, 11, 161.
24. Yao, K. J.; Song, M.; Hourston, D. J.; Luo, D. Z. Polymer 2002, 43, 1017.
25. Lee, S. H.; Kim, J. E.; Song, H. H.; Kim, S. W. Int J Thermophys 2004, 25, 1585.
26. Zhou, H.; Zhang, S.; Yang, M. J Appl Polym Sci 2008, 108, 3822.
27. Benveniste, Y. J Appl Phys 1987, 61, 2840.
28. Hasselman, D. P. H.; Johnson, L. F. J Compos Mater 1987, 21, 508.
29. Nan, C.-W.; Birringer, R.; Clarke, D. R.; Gleiter, H. J Appl Phys 1997, 81, 6692.
30. Kakiage, M.; Takamatsu, R.; Uehara, H.; Yamanobe, T.; Suzuki, K. Key Eng Mater, to appear.
31. Hasegawa, N.; Okamoto, H.; Kato, M.; Usuki, A.; Sato, N. Polymer 2003, 44, 2933.
32. Dong, W.; Zhang, X.; Liu, Y.; Gui, H.; Wang, Q.; Gao, J.; Song, Z.; Lai, J.; Huang, F.; Qiao, J. Eur Polym Mater 2006, 42, 2515.
33. Liff, S. M.; Kumer, N.; McKinley, G. H. Nat Mater 2007, 6, 76.
34. Kumar, N.; Liff, S. M.; McKinley, G. H. US Patent Application 11/253,219.
35. Ando, S.; Sawada, T.; Sasaki, S. Polym Adv Technol 1999, 10, 169.
36. Takahashi, F.; Ito, K.; Morikawa, J.; Hashimoto, T.; Hatta, I. Jpn J Appl Phys 2004, 43, 7200.
37. Yorifuji, D.; Ando, S.; Hashimoto, T. Polym Prep Jpn 2008, 57, 785.
38. Morikawa, J.; Hashimoto, T. J Appl Phys 2009, 105, 113506.
39. Morikawa, J.; Tan, J.; Hashimoto, T. Polymer 1995, 36, 4439.
40. Morikawa, J.; Hashimoto, T. Jpn J Appl Phys 1998, 37, L1484.
41. Morikawa, J.; Hashimoto, T.; Maesono, A. High Temp-High Press 2001, 33, 387.
42. Maesono, A.; Takasaki, Y.; Maeda, Y.; Tye, R. P.; Morikawa, J.; Hashimoto, T. High Temp-High Press 2002, 34, 127.
43. Morikawa, J.; Hashimoto, T. Thermochim Acta 2005, 432, 216.
44. van Olphen, H. An Introduction to Clay Colloid Chemistry, 2nd ed.; Wiley: New York, 1977.
45. Pignon, F.; Magnin, A.; Piau, J. M.; Cabane, B.; Lindner, P.; Diat, O. Phys Rev E 1997, 56, 3281.
46. Saunders, J. M.; Goodwin, J. W.; Richardson, R. M.; Vincent, B. J Phys Chem B 1999, 103, 9211.
47. Jonsson, B.; Labbez, C.; Cabane, B. Langmuir 2008, 24, 11406.
48. Ando, S.; Sawada, T.; Sasaki, S. Polym Adv Technol 2001, 12, 319.
49. Loo, L. S.; Gleason, K. K. Macromolecules 2003, 36, 2587.
50. Loo, L. S.; Gleason, K. K. Polymer 2004, 45, 5933.
51. Cole, K. C.; Perrin-Sarazin, F.; Dorval-Douville, G. Macromol Symp 2005, 230, 1.
52. Ijdo, W. L.; Kemnetz, S.; Benderly, D. Polym Eng Sci 2006, 46, 1031.
53. Chen, G.; Ma, Y.; Zheng, X.; Xu, G.; Liu, J.; Fan, J.; Shen, D.; Qi, Z. J. Polym Sci Part B: Polym Phys 2007, 45, 654.
54. Cole, K. C. Macromolecules 2008, 41, 834.
55. Farmer, V. C.; Russell, J. D. Spectrochim Acta 1964, 20, 1149.
56. Margulies, L.; Rozen, H.; Banin, A. Clays Clay Miner 1988, 36, 476.
57. Johnston, C. T.; Premachandra, G. S. Langmuir 2001, 17, 3712.
58. Kojima, Y.; Usuki, A.; Kawasumi, M.; Okada, A.; Kurauchi, T.; Kamigaito, O.; Kaji, K. J. Polym Sci Part B: Polym Phys 1994, 32, 625.
59. Kojima, Y.; Usuki, A.; Kawasumi, M.; Okada, A.; Kurauchi, T.; Kamigaito, O.; Kaji, K. J. Polym Sci Part B: Polym Phys 1995, 33, 1039.
60. Medellin-Rodriguez, F. J.; Hsiao, B. S.; Chu, B.; Fu, B. X. J. Macromol Sci Part B: Phys 2003, 42, 201.